LA-UR -84-1245
CONF-8404141--1

NOTICE

PORTIONS OF THIS REPORT ARE ILLEGIBLE. It has been reproduced from the best available copy to permit the broadest possible availability.

Los Alamos National Laboratory is operated by the University of California for the United States Department of Energy under contract W-7405-ENG-36.

LA-UR--84-1245

DE84 011370

TITLE: KINETICS OF RED BLOOD CELL AGGREGATION: AN EXAMPLE OF GEOMETRIC POLYMERIZATION

AUTHOR(S): Alan S. Perelson and Richard W. Samsel

SUBMITTED TO: Proceedings International Topical Conference on Kinetics of Aggregation and Gelation, Atlanta, GA, April 2-4, 1984, F. Family and D. P. Landau, eds. North Holland 1984

DISCLAIMER

This report was prepared as an account of work sponsored by an agency of the United States Government. Neither the United States Government nor any agency thereof, nor any of their employees, makes any warranty, express or implied, or assumes any legal liability or responsibility for the accuracy, completeness, or usefulness of any information, apparatus, product, or process disclosed, or represents that its use would not infringe privately owned rights. Reference herein to any specific commercial product, process, or service by trade name, trademark, manufacturer, or otherwise does not necessarily constitute or imply its endorsement, recommendation, or favoring by the United States Government or any agency thereof. The views and opinions of authors expressed herein do not necessarily state or reflect those of the United States Government or any agency thereof.

By acceptance of this article, the publisher recognizes that the U S Government retains a nonexclusive, royalty-free license to publish or reproduce the published form of this contribution, or to allow others to do so, for U S Government purposes.

The Los Alamos National Laboratory requests that the publisher identify this article as work performed under the auspices of the U S Department of Energy

MASTER

Los Alamos
Los Alamos National Laboratory
Los Alamos, New Mexico 87545

FORM NO 836 R4
ST NO 2629 5/81

DISTRIBUTION OF THIS DOCUMENT IS UNLIMITED

KINETICS OF RED BLOOD CELL AGGREGATION: AN EXAMPLE OF GEOMETRIC POLYMERIZATION*

Alan S. PERELSON and Richard W. SAMSEL

Theoretical Division, Los Alamos National Laboratory, Los Alamos, New Mexico 87545, USA, and Division of Biology and Medicine, Brown University, Providence, RI 02912, USA.

The kinetics of the process by which red blood cells aggregate into long cylindrical, and sometimes branched, structures called rouleaux is studied within the framework of both reversible and irreversible addition and condensation polymerization reactions. However, unlike usual polymer kinetics, here we take into account the geometry of the subunits and the geometry of the growing structure. Geometric factors such as the amount of reactive wall area influence the probability of branching and hence the final shape of the aggregate. The inclusion of loop formation reactions is shown to be crucial in obtaining physically realistic equilibrium solutions of the kinetic equations.

1. INTRODUCTION

In the presence of macromolecules, such as fibrinogen or dextran, red blood cells spontaneously aggregate face-to-face to form rouleau -- long, cylindrical shaped objects resembling stacks of coins. At a somewhat lower frequency single red cells, or entire stacks of cells, adhere to the wall of a cylindrical rouleau and form branched treelike structures and ramified networks also called rouleaux. Figure 1 illustrates some typical structures seen early in the aggregation process. Rouleaux constantly form in the microcirculation and dissociate under the influence of high shear forces in large blood vessels. In a variety of disease states the adhesion between red cells is abnormally strong and rouleaux do not break up, leading to blood vessel occlusion. Because of the medical importance of rouleau formation, we have undertaken a number of theoretical studies aimed at predicting the size and shape of rouleaux under idealized conditions (1-4). This work can be considered a first step in determining the conditions under which rouleaux cause circulatory blockages and abnormalties in the rheological properties of blood. For simplicity in setting up tractable models we have assumed collisions among red cells and rouleaux are isotropic and describable by rate constants and mass-action kinetic laws.

A succession of models will be presented. During the early stages of rouleaux formation single cells are the predominant species and hence collisions between single cells and between single cells and small aggregates are the most common events. We thus model this first phase of the reaction as an addition reaction (Section 2). After single cells are depleted, collisions between aggregates predominate. In Section 3 we model this phase of the process by allowing both additon and condensation reactions. When rouleaux get larger than about 10

FIGURE 1
Rouleaux that formed spontaneously in diluted human blood when placed upon a microsope slide.

*Work performed under the auspices of the U.S. Department of Energy. A.S.P. is the recipient of an N.I.H. Research Career Development Award, 5K04-AI00450-05.

cells they have a tendency to branch. In Section 4 a geometric model is introduced. Using this model in Section 5, both the size and degree of branching ("shape") of treelike rouleaux are predicted. Because branching occurs during the later stages of the process, we allow the reactions at this stage of the aggregation process to be reversible. In the final stages of the aggregation process, aggregates either join together and grow so large as to become the equivalent of a gel, or large aggregates become sufficiently separated in space that further reactions between them become unlikely. In either case, free ends within an aggregate react with sites on the aggregate, and loop forming reactions occur. Section 6 discusses some preliminary models of loop formation, followed by a brief conclusion (Section 7).

2. ADDITION MODELS

Consider a monodisperse population of red cells at concentration E_0 that aggregate via irreversible erythrocyte-erythrocyte reactions with rate constant k_e and via irreversible erythrocyte-rouleaux reactions with rate constant k_a. Here we define a rouleau as any aggregate containing two or more red cells. Let E, R, and R(n) be the concentrations of free erythrocytes, total rouleaux, and rouleaux of size n. Then in nondimensional variables one finds

$$dE'/dt' = -kE'^2 - E'R' \quad , \quad E'(0) = 1 \tag{1}$$

$$dR'/dt' = \frac{1}{2} kE'^2 \quad , \quad R'(0) = 0 \tag{2}$$

$$dR'(2)/dt' = \frac{1}{2} kE'^2 - E'R'(2), \quad R'(2,0) = 0 \tag{3}$$

$$dR'(n)/dt' = E'[R'(n-1) - R'(n)], \; R'(n,0) = 0 \tag{4}$$

where $k = k_e/k_a$, $E' = E/E_0$, $R' = R/E$, $R'(n) = R(n)/E_0$ and $t' = k_a E_0$. Although these equations cannot be solved explicitly, one finds for $k = 2$, that the substitution $U = 1/(E'+R')$ leads to the results (1)

$$E' = U^{-1}(1-\ln U) \tag{5}$$

and

$$t' = e[E_1(1-\ln U) - E_1(1)] \tag{6}$$

where $E_1(1)$ is the exponential integral of order 1 and e is the base of the natural logarithms. Solving Eq. (6) for $U(t')$, either asymptotically or numerically, allows one to find $E'(t')$ from Eq. (5) and hence $R'(t')$ and $R'(n,t')$. In particular, in the limit $t' \to \infty$, $E' \to 0$, hence $U \to e$ and $R' \to 1/e$. Further results based on numerical studies are reported in (1).

When $k \neq 2$, Hendriks and Ernst (5) have shown that a related procedure can be used. Reparameterizing time so that

$$d\tau = E'(t')dt' \quad , \tag{7}$$

Eqs. (1)-(4) become a linear system that can be solved in a straightforward manner for $E'(\tau)$, $R'(\tau)$ and $R'(n,\tau)$. However, to find the solutions as a function of t', one needs to evaluate the integral.

$$t' = \int_0^\tau [E'(\tau')]^{-1} d\tau' \quad . \tag{8}$$

When $k = 2$, this integral reduces to Eq. (6) and one finds $\tau = \ln U$.

For $0.1 \le k \le 10$, a range that spans most biologically reasonable values, the mean size of an aggregating unit, U, where a unit is either a single cell or a rouleaux, approaches a value close to 3 (1). In many experiments only small aggregates in this size class form (6,7), and qualitative agreement between theory and experiment is found. However, as shown in Fig. 1, much larger rouleaux commonly occur. From this we deduce that collisions among rouleaux must be significant. Moreover, collisions between rouleaux leading to large aggregates have been observed (1).

3. CONDENSATION MODELS

Modifying the addition theory by including a condensation reaction with rate constant k_c, one finds

$$dE/dt = -k_e E^2 - k_a ER \tag{9}$$

$$dR/dt = \frac{1}{2} k_e E^2 - \frac{1}{2} k_c R^2 \tag{10}$$

$$dR(2)/dt = \frac{1}{2} k_e E^2 - k_a ER(2) - k_c R(2) \sum_{m=2}^{n-2} R(m) \tag{11}$$

$$dR(n)/dt = k_a E[R(n-1)-R(n)] + \frac{1}{2} k_c \sum_{m=2}^{n-2} R(n-m)R(m) - k_c R(n) \sum_{m=2}^{\infty} R(m) \quad , \quad n = 3,4,\ldots \tag{12}$$

When $k_e = k_a = k_c$, these equations reduce to the Smoluchowski coagulation equation with R(1) replaced by E. Numerical studies of Eqs. (9)-(12) are reported in (1) and some analytic results in (5). Comparison with our data (1) indicates that $k_c < k_e$ and $k_c < k_a$.

4. AN IDEALIZED GEOMETRIC MODEL

To predict the degree of branching in rouleaux a different class of models is needed that includes geometric information. These are described briefly below and more fully in (1) and (4).

Consider a red blood cell to be a cylindrical disk of radius r and height h, with two faces

each having surface area $e = \pi r^2$ and a wall having surface area $w = 2\pi rh$. The average diameter of a human red cell is approximately 8μm and $h/r = .62$. Thus, the disk representing a red cell is about one third as high as it is wide. Red cells adhere face-to-face to form cylindrical stacks, the surface area of which can easily be calculated.

The cylindrical shape of rouleaux is due in part to a realignment of cells that occurs after cell-cell contact is made. A stack increases in length when a red cell adheres to a small elongation zone at the end of the stack. Because red cells are flexible and are able to move relative to one another, the elongation zone comprises the exposed face of the last cell in the stack and a portion of the adjoining wall. A cell that adheres to this portion of the wall will move to the end of the stack and orient itself so that it adheres face to face. Photographs of the various stages in this process are presented in (1).

The two elongation zones at the free ends of a stack are called <u>caps</u> because they resemble the cap on an object such as a fountain pen. The area of a cap, a_c, is a parameter in the model that can be chosen so that the cap is the end of the stack (i.e., $a_c = e$) or a true elongation zone (e.g., $a_c = e+w$). A branched rouleau is modeled as an aggregate of linear stacks called <u>segments</u> connected at right angles.

We first study rouleaux containing no loops. Such rouleaux can be characterized by n, the number of cells they contain and c, their number of caps. By definition, a rouleau contains two or more cells, $n \geq 2$. Let $R(n,c)$ be the concentration of treelike rouleaux with n cells and c caps. Using this description of rouleaux we have no information about the length of the various segments comprising a rouleau. Thus we also compute $S(n,c)$, the concentration of segments within rouleaux containing n cells and c caps. A segment has at most 2 free ends and thus for segments $c \leq 2$.

5. KINETICS OF GROWTH

5.1. Variables

Assume treelike rouleaux grow and decay by the reversible polycondensation and addition reactions shown in Fig. 2. Loop forming and wall-wall reactions are ignored for the present. We describe the growth of rouleaux at two levels --first, in terms of the following macroscopic descriptors of the process from which one can determine the mean size and shape of rouleaux:

- E - the concentration of erythrocytes
- R - the concentration of rouleaux (aggregates containing two or more cells)
- S - the concentration of segments within rouleaux
- M - the concentration of caps on rouleaux
- W - the concentration of reactive wall area (non-cap surface area) on rouleaux
- T - the total concentration of surface area in rouleaux

--and second, in terms of the complete distributions $S(n,c)$ and $R(n,c)$.

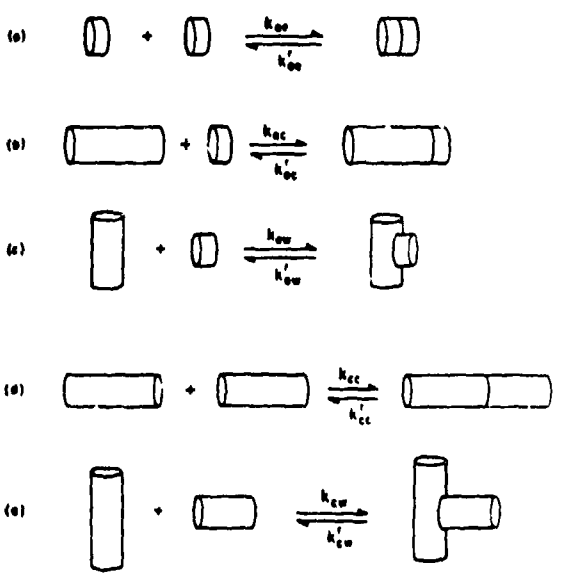

FIGURE 2

Diagrammatic representation of reactions that generate rouleaux. (a) Two erythrocytes react with rate constant per unit area k_{ee}. (b) An erythrocyte reacts with the cap on a rouleau with rate constant per unit area k_{ec}. This reaction elongates the rouleau. (c) An erythrocyte reacts with the wall of a rouleau to initiate a branch with rate constant k_{ew}. (d) Two rouleaux react via a cap-cap interaction with rate constant per unit area k_{cc}. (e) Two rouleaux react via a cap-wall interaction with rate constant k_{cw}. The reverse reactions and their rate constants are also shown. (Reproduced with permission from Ref. (4)).

5.2 Macroscopic Equations

The macroscopic variables obey the following equations

$$dE/dt = - k_{ee}a_eE^2 - k_{ec}a_cME - k_{ew}EW$$

$$+ 2k^r_{ee}S(2,2) + k^r_{ew}S(1,1)$$

$$+ k^r_{ec} \sum_{c=0}^{2} \sum_{n=c+1}^{\infty} cS(n,c) \quad . \qquad (13)$$

$$dM/dt = k_{ee}a_eE^2 + k_{ew}EW - k_{cc}a_cM^2 - k_{cw}MW$$

$$- 2k^r_{ee}S(2,2) - k^r_{ew}S(1,1)$$

$$+ 2k^r_{cc}\sum_{c=0}^{2}\sum_{n=c+1}^{\infty}(n-c-1)S(n,c)$$

$$+ k^r_{cw}\sum_{c=0}^{2}\sum_{n=c+1}^{\infty}(2-c)S(n,c) \quad . \qquad (14)$$

$$dW/dt = (w-a_c+e)k_{ee}a_eE^2 + wk_{ec}a_cME + (w-a_c)k_{ew}EW$$

$$+ (a_c-e)k^2_{cc}a_cM^2 + (a_c-2e)k_{cw}MW$$

$$- 2(w-a_c+e)k^r_{ee}S(2,2) - (w-a_c)k^r_{ew}S(1,1)$$

$$- wk^r_{ec}\sum_{c=0}^{2}\sum_{n=c+1}^{\infty}cS(n,c)$$

$$- 2(a_c-e)k^r_{cc}\sum_{c=0}^{2}\sum_{n=c+1}^{\infty}(n-c-1)S(n,c)$$

$$- (a_c-2e)k^r_{cw}\sum_{c=0}^{2}\sum_{n=c+1}^{\infty}(2-c)S(n,c) \qquad (15)$$

$$S = (1/2e)[(E_0-E)w + (2e-a_c)M - W] \quad . \qquad (16)$$

$$T = W + Ma_c \quad . \qquad (17)$$

and

$$R = M - S \quad . \qquad (18)$$

where E_0 is the total concentration of erythrocytes in the system, and the rate constants are defined in Fig. 2. The forward rate constants governing collisions between rouleaux are all given in units of concentration^{-1} per unit area per unit time. Thus the area of a cap, a_c, erythrocyte a_e, wall of an erythrocyte w, and the face or end of an erythrocyte, e, all enter the equations. By separating out these geometric factors from the basic forward rate constants we can independently study the effects of geometry and collision rate. The equation for W is the most novel in that it keeps track of the gain or loss of wall area in rouleaux for each reaction depicted in Fig. 2. Detailed deviations of these equations are given in Samsel and Perelson (1). For illustrative purposes we indicate how Eq. (13) is derived. The forward reaction terms describe the loss of free erythrocytes by collision with other erythrocytes, by collision with a cap, and by collision with a wall of a rouleaux. The reverse reaction terms describe the dissociation of a two-cell rouleau [i.e., $S(2,2)$] contributing two free cells, the dissociation of a one-cell segment from a wall, and the dissociation of the terminal cell on a segment containing one or two caps.

Under the assumption that the five rate constants for the reverse reactions shown in Fig. 2 are equal, one can evaluate the summations in Eqs. 13-15. If we define k_r so that

$$k_r \equiv k^r_{ee} = k^r_{ec} = k^r_{ew} = k^r_{cc} = k^r_{cw} \quad . \qquad (19)$$

it is easy to show that

$$dE/dt = - k_{ee}a_eE^2 - k_{ec}a_cME - k_{ew}EW + k_rM \qquad (20)$$

$$dM/dt = k_{ee}a_eE^2 + k_{ew}EW - k_{cc}a_cM^2 - k_{cw}MW$$

$$+ 2k_r(E_0-E) - 3k_rM \quad . \qquad (21)$$

and

$$dW/dt = (w-a_c+e)k_{ee}a_eE^2 + wk_{ec}a_cME + (w-a_c)k_{ew}EW$$

$$+ (a_c-e)k_{cc}a_cM^2 + (a_c-2e)k_{cw}MW +$$

$$+ k_r(w - 2a + 2e)(E_0-E-M) - k_rW \quad . \qquad (22)$$

While the reverse reaction terms in Eqs. 20-22 are surprisingly simple when compared with the corresponding terms in Eqs. 13-15, they do not seem to be intuitively transparent.

5.3 Microscopic Equations for $S(n,c)$

The growth and decay of segments within rouleaux are easily describable (4). For the case in which all the reverse rate constants are equal, one finds

$$dS(1,1)/dt = k_{ew}EW - k_{ec}a_cES(1,1)$$

$$- k_{cc}a_c MS(1,1) - k_{cw}WS(1,1)$$

$$+ k_r \{2S(1,0) - S(1,1)$$

$$+ \sum_{n=2}^{\infty} [2S(n,0) + S(n,1)]\} \quad . \qquad (23)$$

$$dS(2,2)/dt = \frac{1}{2} k_{ee}a_e E^2 - 2k_{ec}a_c ES(2,2)$$

$$- 2k_{cc}a_c S(2,2)M - 2k_{cw}S(2,2)W$$

$$+ k_r\{S(2,1) - S(2,2)$$

$$+ \sum_{n=3}^{\infty} [S(n,1) + 2S(n,2)]\} \quad . \qquad (24)$$

$$dS(n,0)/dt = k_{cw}WS(n,1) + \frac{1}{2} k_{cc}a_c \sum_{k=1}^{n-1}$$

$$\times S(k,1)S(n-k,1) - k_r(n+1)S(n,0) \quad . \qquad (25)$$

$$dS(n,1)/dt = k_{ec}a_c E[S(n-1,1) - S(n,1)]$$

$$+ 2k_{cc}a_c \sum_{k=2}^{n-1} S(k,2)S(n-k,1)$$

$$- k_{cc}a_c MS(n,1)$$

$$+ k_{cw}W[2S(n,2) - S(n,1)]$$

$$+ k_r[\sum_{k=n+1}^{\infty} S(k,1) + 2 \sum_{k=n}^{\infty} S(k,0)] \qquad (26)$$

$$dS(n,2)/dt = 2k_{ec}a_c E [S(n-1,2) - S(n,2)]$$

$$+ 2k_{cc}a_c \sum_{k=2}^{n-2} S(k,2)S(n-k,2) \quad ,$$

$$- 2k_{cc}a_c S(n,2)M - 2k_{cw}WS(n,2)$$

$$+ k_r\{ \sum_{k=n}^{\infty} [S(k,1) + 2S(k,2)] - nS(n,2)\} \qquad (27)$$

5.4 Detailed Balance

Using the principle of detailed balance one can show (1) that the five forward rate constants are not independent. In fact, one finds that

$$k_{cc} = \frac{k_{ec}^2 a_c}{k_{ee}a_e} \qquad (28)$$

and

$$k_{cw} = \frac{k_{cw}k_{ec}a_c}{k_{ee}a_e} \qquad (29)$$

If we view a red cell as a segment of length one with two caps, then either of these two caps could attach to the end of a growing segment in a typical cap-cap reaction. Hence we assume

$$k_{ec} = 2k_{cc} \quad . \qquad (30)$$

As a consequence of Eqs. (28)-(30) we need only define two forward rate constants

$$k_c \equiv k_{cc} = k_{ec}/2 = k_{ee}a_e/4a_c \quad , \qquad (31a)$$

and

$$k_w \equiv k_{cw} = k_{ew}/2 \quad , \qquad (31b)$$

where k_c is the rate constant for elongation reactions and k_w the rate constant for branching reactions.

5.5 An Exact Solution

Viewing each face of a red cell as a reactive site, we can use probablistic methods, á la Flory (8), to solve Eqs. (23)-(27) with the rate constants chosen as in Eq. (31). As shown in (4), we find

$$S(n,0) = E_0 p_w^2 p^{n-1} \quad , \quad n = 1,2,... \qquad (32a)$$

$$S(n,1) = 2E_0 p_f p_w p^{n-1} \quad , \quad n = 1,2,... \qquad (32b)$$

$$S(n,2) = E_0 p_f^2 p^{n-1} \quad , \quad n = 2,3,... \qquad (32c)$$

where

$$p_f = \frac{2E + M}{2E_0} \tag{33a}$$

$$p_w = \frac{2S - M}{2E_0} \tag{33b}$$

$$p = \frac{E_0 - E - S}{E_0} \tag{33c}$$

and E, S, and M are given by the solutions to Eqs. (20)-(22) and (16)-(18). Rather than determining how E, S, and M vary with time by solving the differential and algebraic equations (20)-(22) and (16)-22), one can, by differentiating Eq. (33) and making various substitutions, determine that p_f and p_w and p satisfy the following equations:

$$\frac{dp_f}{dt} = - k_w E_0(2a_c-2e-w)p_f^3 + 2E_0[k_w(a_c-e) - k_c a_c]p_f^2 - (k_w E_0 w+k_r)p_f + 2ek_w E_0 p_f p_w + k_r \quad , \tag{34a}$$

$$\frac{dp_w}{dt} = k_w E_0(2a_c-2e-w)p_f^3 - 2k_w E_0(a_c-e)p_f^2 + wk_w E_0 p_f - 2ek_w E_0 p_f p_w - k_r p_w \quad , \tag{34b}$$

and p may be determined from

$$p(t) = 1 - p_f(t) - p_w(t) \quad . \tag{34c}$$

Further one can show that (4):

$$E = E_0 p_f^2 \tag{35a}$$

$$S = E_0(p_f + p_w - p_f^2) \tag{35b}$$

$$M = 2E_0 p_f(1 - p_f) \tag{35c}$$

$$R = E_0(p_f - p_w - p_f^2) \tag{35d}$$

and

$$W = E_0[w(1 - p_f^2) - 2a_c p_f(1 - p_f) + 2e(p_f - p_w - p_f^2)] \quad . \tag{35e}$$

Numerical solutions of Eqs. (34) and (35) are given in (4). From these solutions one can determine various mean quantities describing the rouleau size and shape distribution such as

$\langle n\rangle_r$ = $(E_0-E)/R$, the mean number of cells per rouleau

$\langle n\rangle_s$ = $(E_0-E)/S$, the mean number of cells per segment,

$\langle n\rangle_u$ = $E_0/(E+R)$, the mean number of cells per unit, (36)

$\langle n\rangle_{su}$ = $E_0/(E+S)$, the mean number of cells in a straight chain unit,

$\langle b\rangle$ = S/R, the mean number of branches or straight segments per rouleau,

and

$\langle c\rangle$ = M/R, the mean number of caps per rouleau.

In (4) we present detailed studies of how these mean quantities change with respect to the blood hemotocrit ($\sim E_0$), and the rate constants k_r, k_w, and k_c over the biologically relevant parameter ranges. Comparisons with data are also given. We find that by choosing the appropriate parameter values, our model generates good fits to existing data. However, very detailed data about the aggregate size distribution, especially when the aggregates grow large, does not yet exist.

Forming the kinetic equations for R(n,c) is a more complex matter. Samsel and Perelson (1) derive the appropriate equations under the assumption that the aggregation process is irreversible.

In the presence of fragmentation, the forward reaction equations combined with the equilibrium solution (2,3) and the principle of detailed balance, can be used to construct the appropriate fragmentation terms (9). Van Dongen and Ernst (10,11) demonstrate this procedure in the context of a simplified rouleau model, and hence it will not be dealt with here.

5.7 Equilibrium Solution

Setting the time derivatives to zero in Eq. (34) allows one to find the equilibrium values of p_f, p_w, and p and hence the equilibrium values of all the macroscopic variables E, M, W, S, T, and R, and the mean quantities given in Eq. (36). Detailed studies of the equilibrium solution are presented elsewhere (4).

When k_w/k_c is large and the reverse rate constant k_r low, our numerical studies show that aggregates grow infinitely large (Fig. 3) signaling the occurrence of a sol-gel phase transition. If we use our model to compute equilibrium solutions past the gel point, we find

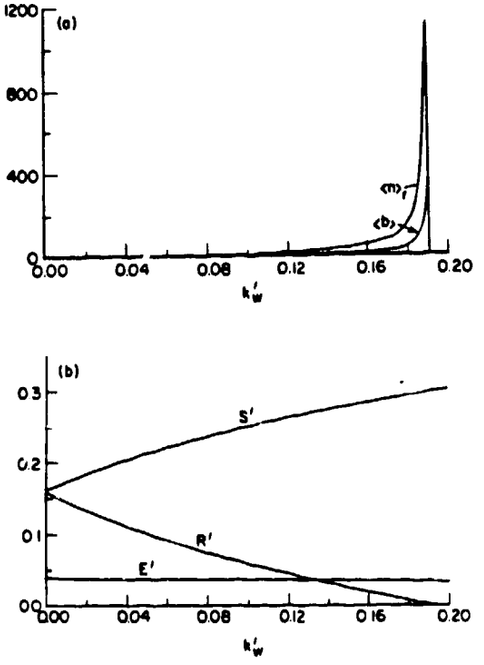

FIGURE 3

Equilibrium solution of the reversible rouleaux equations exhibit a divergence similar to a sol-gel transformation when $k' = k_w w/k_c a_c$ reaches a critical value. Here $k'_r = k_r/k_c a_c E_0 = 0.1$. Note in (a) that both $\langle n \rangle_r$, the mean number of cells per rouleau, and $\langle b \rangle$, the mean number of branches per rouleau, $\to \infty$ as the nondimensional equilibrium concentration of rouleaux $R' = R/E_0 \to 0$ in (b). (Reproduced from Ref. (4) with permission).

the concentration of rouleaux is negative. The reason is simple: if the total concentration of caps is positive, the model predicts that cap-cap or cap-wall adhesions occur, thus reducing the number of free rouleaux even if all cells are in one infinite aggregate. From Eqs. (16)-(18) and (20)-(22) one finds

$$dR/dt = \frac{1}{2} k_{ee} a_e E^2 - \frac{1}{2} k_{cc} a_c M^2 - k_{cw} MW + k_r(E_0 - E - M - R) \quad . \tag{37}$$

Thus as E and R approach zero with $M > 0$ the negative terms dominate, and $dR/dt < 0$. We thus can use $R < 0$ as a criteria for being past the gel point.

In our experiments we generally do not see infinitely large aggregates. Rather the concentration of free caps appears to be reduced by loop formation.

6. LOOP FORMATION

6.1 Mechanisms of Loop Formation

The final stage of rouleau formation is characterized by the presence of large aggregates with many caps. In a fluid the segments within rouleaux move and are sufficiently flexible to form cyclic structures (see Fig. 1). Loops can be formed when two caps join or when a cap encounters a wall and sticks to it. A loop may also be formed when the wall on a flexible segment folds back and joins to another segment of wall on the rouleau. Keeping track of the amount of reactive wall area annihilated in such wall-wall reactions is a difficult and yet unresolved problem. Loop forming cap-cap and cap-wall reactions can be incorporated into our kinetic model. Here we indicate one way in which this may be done. In a future publication we plan to discuss a number of alternative models for loop formation.

6.2 A Simple Model

Loop formation is a reaction that takes place within individual rouleaux. Using macroscopic variables we can describe loop formation in an average sense. The average number of caps per rouleaux is M/R. Assuming that in the neighborhood of every cap there is a constant density of other caps, and that the caps lie on segments that are sufficiently flexible that the length of the segment is irrelevant in determining the motion of the cap, then the average rate of cap-cap reactions can be expressed as

$$k_{\ell c} a_c R(\frac{M}{R})(\frac{M}{R} - 1) H(\frac{M}{R} - 1) \quad , \tag{38}$$

where $k_{\ell c}$ is the forward rate constant for loop forming cap-cap reactions and $H(\cdot)$ is a heavy-side function included to insure that cap-cap reactions are only considered when the average number of caps per rouleau is greater than one. To model the situation in which cap-cap reactions are only important when the average number of caps per rouleau is large, say $M/R > c_{min} >> 1$, one can replace Eq. (38) by

$$k_{\ell c} a_c \frac{M^2}{R} H(\frac{M}{R} - c_{min}) \quad , \tag{39}$$

Loops can also form by cap-wall reactions. The concentration of reactive wall per rouleau is W/R, and thus by analogy with the above derivation, the rate at which loops form by cap-wall reactions is

$$k_{\ell w} W \frac{M}{R} H(\frac{W}{R} - w_{min}) \quad , \tag{40}$$

where $k_{\ell w}$ is the forward rate constant characterizing cap-wall loop forming reactions and w_{min} is the minimum wall area required before such reactions need be considered.

By including loop forming reactions in our basic model $M \to 0$ as $R \to 0$. (To see this, notice that the rate of loop forming reactions that destroy caps becomes unbounded as $R \to 0$.) Thus R never goes negative, and our model remains valid for all parameter values. These models for loop formation are very simple, but yet illustrate the major point that loops become common as aggregates grow large, i.e., $R \to 0$.

7. CONCLUSIONS

Determining the size and shape of red cell aggregates that can form in the circulation is an important practical medical problem. Here we have tried to show via idealized models that, by including geometric factors in polymerization reactions corresponding to collision cross-sections, one can keep track of both the size and degree of branching of rouleaux that develop under conditions of isotropic, random collisions. Our models are examples of analytic attempts to understand cluster-cluster aggregation by combining polymerization kinetics with geometry.

ACKNOWLEDGEMENTS

I would like to thank Carol England for her assistance in preparing the camera-ready copy and Schwartz, Davenport & Schwendimann for the kind use of their quiet offices in preparing an initial draft.

REFERENCES

(1) R.W. Samsel and A.S. Perelson, Biophys. J. 37 (1982) 493.
(2) R.W. Samsel and A.S. Perelson, Biophys. J. 37 (1982) 515.
(3) F.W. Wiegel and A.S. Perelson, J. Stat. Phys. 29 (1982) 813.
(4) R.W. Samsel and A.S. Perelson, Biophys. J in print.
(5) E.M. Hendriks and M.H. Ernst, J. Colloid Interface Sci. 97 (1984) 176.
(6) M. Herbst and J.H. Goldstein, this volume.
(7) D. Kernick, A.W.L. Jay, S. Rowlands and L. Skibo, Can. J. Physiol. Pharmacol. 51 (1973) 690.
(8) P. Flory, "Principles of Polymer Chemistry" (Cornell Univ. Press, Ithaca, 1953).
(9) P.G.J. van Dongen and M.H. Ernst, J. Phys. A: Math. Gen. 16 (1983) L327.
(10) P.G.J. van Dongen and M.H. Ernst, this volume.
(11) P.G.J. van Dongen and M.H. Ernst, J. Stat. Phys., in print.